Published in final edited form as:
Neuroimage. 2006 January 15; 29(2): 452–466. doi:10.1016/j.neuroimage.2005.07.048.

Cytology and Functionally Correlated Circuits of Human Posterior Cingulate Areas

Brent A. Vogt[1], **Leslie Vogt**[1], and **Steven Laureys**[2]

1 *Cingulum NeuroSciences Institute & SUNY Upstate Medical University, 750 E. Adams Street, Syracuse, NY 13210*

2 *Department of Neurology, CHU Sart Tilman and Cyclotron Research Centre, University of Liège, 4000 Liège, Belgium*

Abstract

Human posterior cingulate cortex (PCC) and retrosplenial cortex (RSC) form the posterior cingulate gyrus, however, monkey connection and human imaging studies suggest that PCC area 23 is not uniform and atlases mislocate RSC. We histologically assessed these regions in 6 postmortem cases, plotted a flat map, and characterized differences in dorsal (d) and ventral (v) area 23. Subsequently, functional connectivity of histologically guided regions of interest (ROI) were assessed in 163 [^{18}F] fluorodeoxyglucose human cases with PET. Compared to area d23, area v23 had a higher density and larger pyramids in layers II, IIIc, and Vb and more intermediate neurofilament-expressing neurons in layer Va. Coregisrtration of each case to standard coordinates showed that the ventral branch of the splenial sulci coincided with the border between d/v PCC at −5.4±0.17 cm from the vertical plane and +1.97±0.08 cm from the bi-commissural line. Correlation analysis of glucose metabolism using histologically guided ROIs suggested important circuit differences including dorsal and ventral visual stream inputs, interactions between the vPCC and subgenual cingulate cortex, and preferential relations between dPCC and the cingulate motor region. The RSC, in contrast, had restricted correlated activity with pericallosal cortex and thalamus. Visual information may be processed with an orbitofrontal link for synthesis of signals to drive premotor activity through dPCC. Review of the literature in terms of a PCC duality suggests that interactions of dPCC, including area 23d, orients the body in space via the cingulate motor areas, while vPCC interacts with subgenual cortex to process self-relevant emotional and non-emotional information and objects and self reflection.

Keywords

Cingulate cortex; cytoarchitecture; retrosplenial cortex; neurofilament proteins; glucose metabolism; cerebral cortex; self reflection

Introduction

The primate posterior cingulate gyrus is comprised of ventral bank retrosplenial areas 29 and 30 (RSC) and posterior cingulate areas 23 and 31 (PCC) including an extension into the cingulate sulcus. According to stroke and functional imaging in humans and single neuron electrophysiology in monkey, this region plays a role in memory access and visuospatial orientation. Strokes in right hemisphere RSC/PCC can produce topographic disorientation

Corresponding author: Brent A. Vogt, Ph.D., Cingulum NeuroSciences Institute, 4435 Stephanie Drive, Manlius, NY 13104, 315-280-6847, bvogt@twcny.rr.com.

(Takahashi et al., 1997) as did a splenial glioma (Bottini et al., 1990), while those in the left hemisphere and tumors pressing preferentially on the left RSC produced severe anterograde and retrograde memory impairments including that for verbal and visual information (Valenstein et al., 1987; Rudge and Warrington, 1991). Functional imaging has shown this region is part of a network that mediates topokinetic (spatial) navigation and memory (Ghaem et al., 1997; Maguire et al., 1997; Berthoz, 1997, 1999). Alert monkey studies by Olson et al. (1993, 1996) showed that neurons in the dorsal PCC were active while assessing large visual field patterns and activity was tightly linked to the position of the eye in the orbit and the direction and amplitude of saccadic eye movements. Finally, lesions of the anterior thalamic nuclei, which project to RSC, disrupt object-in-place memory in monkeys, although cingulate gyrus ablations did not (Parker and Gaffan, 1997). Taken together, it appears that RSC and its thalamic afferents have a role in accessing long-term memories including those associated with spatial orientation, while PCC is involved in topokinesis and related memories.

Functional imaging studies frequently activate PCC during facial and word recognition tasks which might conflict to some extent with the above noted conclusion relating to visuospatial orientation. An evaluation of the extent to which different cingulate subregions are activated by emotional words and faces showed that anterior and midcingulate cortices were activated only by stimuli expressing emotion, while vPCC was activated by both emotion-expressing and non-emotional stimuli (Vogt et al., 2003). For example, happiness generated by personally relevant memory and facial expressions activate vPCC (George et al., 1996; Phillips et al., 1998; Damasio et al., 2000); however, non-emotional conditions also activate this region (Fink et al., 1996; Maguire and Mummery, 1999; Shah et al., 2001; Bernstein et al., 2002). Furthermore, studies of self-reflection and self-imagery activate the vPCC (Kircher et al., 2001, 2002; Johnson et al., 2002; Phan et al., 2003; Sugiura et al., 2005) and this may be pivotal to understanding the overall information processing functions of this region. Thus, the role of this region in topokinesis may be related to the egocentric orientation of the body in relation to external landmarks as well as faces and words with particular and personal meanings.

One intriguing aspect of functional imaging findings discussed above is that words, faces, and self-reflection activate the vPCC including the caudomedial subregion (Vogt et al., 2003). The caudomedial subregion is located on the ventral bank of the cingulate gyrus (Vogt et al., 2001, 2004) and has direct projections to subgenual ACC; connections that dorsal PCC and posterior MCC do not have (Vogt and Pandya, 1987). Furthermore, Shibata and Yukie (2003) reported that the dorsal and ventral parts of PCC have unique thalamic connections with the dPCC receiving inputs from the central latocellular, mediodorsal, and ventral anterior and ventral lateral nuclei that do not project to the vPCC. The structural duality of PCC has also been reported in monkey brain (Vogt et al., 2005). Thus, anatomical and functional studies suggest that PCC is heterogeneous and its subdivisions interact differently with ACC.

The cytology and circuitry observations in monkey led us to formulate three hypotheses. First, the human dPCC and vPCC have qualitatively unique cytological organizations when viewed with antibodies that label proteins in neuronal somata and proximal dendrites. Second, these two areas should have substantially different connections. To test this hypothesis, the border between each division could be identified and the subareas were used as independent regions of interest to seed correlation analyses in resting glucose metabolism for an assessment of their functional connectivity with [^{18}F]fluorodeoxyglucose positron emission tomography (FDG-PET). Based on the thalamocortical and corticocortical connections in monkey, we predicted that correlated activity would differ in both cortex and thalamus and these expectations could be evaluated with well known monkey connections such as those between anterior cingulate cortex (ACC; Vogt and Pandya, 1987) and vPCC. Finally, RSC has thalamic inputs that arise mainly from the anterior thalamic nuclei and differ substantially from those in PCC (Vogt et al., 1987) and RSC is heavily connected with adjacent area 23 (Vogt and Pandya, 1987). We

predicted a heavy thalamic engagement with seeding limited to RSC and heavy correlations with PCC. A final goal of this work was to evaluate the extent to which differences in circuitry uncovered by the correlation analysis provide a basis for evaluating the mechanisms of their differential functions. Since the literature has not been assessed from the perspective of two divisions of PCC, a consideration of the functions of each subdivision was undertaken.

The results confirmed the first hypothesis by showing a structural dichotomy in the human PCC similar to that in monkey. The differential visual inputs to d/vPCC were not predicted, although they are compatible with the current assessment of the functional imaging literature. Demonstration of interactions of vPCC with ACC and those of dPCC with premotor, dorsal visual, and orbitofrontal regions all conform to well-established connections in monkey brain. Interestingly, however, in spite of the heavy connections between RSC and PCC, the correlated voxels were limited to the ventral part of the cingulate gyrus and thalamus. These findings lead to new perspectives on the structure, connections and functions of PCC in terms of functional units rather than a homogeneous posterior cingulate region with a single organization and function.

Materials and Methods

Histological Preparations

Six brains were used that had complete cingulate gyrus staining (below) and the characteristics of each case have been reported (Vogt et al., 2003). There were 4 males and 2 females, ages of 52±2.7 years, brain weights of 1279±67 g, postmortem intervals of 10.8±2.5 hrs and causes of death as follows: carcinoma (3); pneumonia (1), midbrain stroke (1), congestive heart failure (1). All brains were obtained from the Office of the Chief Medical Examiner in cooperation with the Chief of Neuropathology in the Department of Pathology at Wake Forest University School of Medicine (Winston-Salem, NC). The brains were part of a family-approved autopsy procedure that included brain assessment prior to the present analyses. All cases were established as cognitively normal based on medical records and telephone interviews with close family members to establish the level of job and family functioning just prior to death. A neuropathological analysis, including deposition of amyloid beta peptides, neurofibrillary tangles, Lewy bodies, and neurodegeneration, confirmed that cingulate cortex was normal. A *post hoc* analysis was performed on a case cut in the horizontal plane to view borders identified in the 5 coronal cases. This subject was a heavy smoker and two months before death he had an unconscious episode. Although there was diffuse glia in the cerebral cortex; neuronal and laminar architectures are normal in the cingulate gyrus and all thionin-stained neurons were NeuN-positive.

The medial cortex was photographed for all cases, 5 cases were cut coronally into 8–42 blocks and one was cut horizontally, and all were re-photographed. The blocks were immersion fixed in either 10% formalin (n=1) or 4% paraformaldehyde (n=5). The former case had been fixed for about 6 months and embedded in celloidin, while the latter five were fixed for 3–5 days and cryoprotected in sucrose for immunohistochemistry. Every block from all cases was sectioned into six alternating series and one series each used for thionin, neuron-specific nuclear binding protein (NeuN), non-phosphorylated intermediate neurofilaments (SMI32), and calretinin. Sections were pretreated with 75% methanol/7.5% hydrogen peroxide, followed by a 3 min pretreatment with formic acid (NeuN only) and then a washing with distilled water and two washes in phosphate buffered saline (PBS). Sections were incubated in primary antibody in PBS (SMI32, Sternberger Monoclonals, Lutherville, MD, 1:10,000 dilution, mouse; NeuN, Chemicon, Temecula, CA, 1:1,000 dilution, mouse; calretinin, 1:3,000 dilution, mouse, Chemicon) containing 0.3% Triton X-100 (Sigma, St. Louis, MO) and 0.5 mg/ml bovine serum albumin (Sigma) overnight at 4°C. Sections were rinsed in PBS and incubated in biotinylated secondary antibody at 1:200 in PBS/Triton-X/bovine serum albumin for one

hour. Following rinses in PBS, sections were incubated in ABC solution (1:4; Vector) in PBS/Triton-X/bovine serum albumin for one hour followed by PBS rinses and incubation in 0.05% diaminobenzidine (Sigma), 0.01% H_2O_2 in a 1:10 dilution of PBS for 5 min. After PBS rinses, the sections were mounted, dried, thionin (Fisher Scientific, Pittsburgh, PA) counterstained (3 min; 0.05% in 3.7% sodium acetate, 3.5% glacial acetic acid, pH 4.5), dehydrated, and coverslipped.

Data Analysis

There were five steps for the histological analysis. First, sections at a 1–2 mm interval were macrophotographed at 1X with a MacroFire digital camera (Optronics, CA). Second, each section was microscopically scanned to assess the structure of areas in terms of differences in cytoarchitecture along the full extent of area 23. Third, the Talairach and Tournoux coordinates, callosal sulcus, and anterior commissure of their case (1988; their Figure 42) was fitted to the medial surface digital photograph of each postmortem case using two separate layers in Adobe Photoshop 6.0 software (San Jose, Ca). Each case was aligned by reducing the opacity of the Talairach and Tournoux image to 50% so the underlying brain could be observed. The case and coordinate system were then aligned using the anterior commissures, the rostral, dorsal, and caudal edges of the corpora callosa and the cingulate sulci as fiducials. This was a two-dimensional co-registration and it was not necessarily uniform; i.e., both dimensions were warped where needed to align the fiducials of each case to Talairach coordinates. Although the fitting was not uniform, one of the benefits of using the medial surface alone is that adjustments to accommodate the entire lateral surface in whole-brain coregistrations were not required and this enhanced the accuracy of medial surface coregistrations. Fourth, 2–5 microphotographs were taken from all blocks, depending on their length in the A/P plane, through layers III-VI at 150X and they were printed together for each case. Fifth, the photographs were used to guide a final assessment of where the borders of each region were located in the coregistrations so measurements from the vertical plane at the anterior commissure (VCA) could be determined and a population mean±SEM calculated. This variance is a measure of the variability of the histological border.

Regional flat map and standardized coordinates

Approximately half of PCC is in sulci and to expose this cortex for definition of cytoarchitectural borders, the posterior cingulate gyrus was flattened in two dimensions as in Figure 1 according to the following steps: a) Thirteen sections were macrophotographed at 1X as discussed above at about 0.3 cm intervals throughout the posterior cingulate gyrus. b) The distance between adjacent sulcal fundi and gyral vertices (dorsal and ventral apex of the gyral surface) were measured at the layer IV/Va border. c) The corpus callosum (cc) was drawn from the medial surface photograph into a digital file and each section aligned to it and dots placed at each measured distance dorsal to the cc. d) The dots were connected to form the cingulate gyrus dorsal bank, surface and ventral bank. This map is a one-dimensional map in the plane of the arrow in Figure 1 pointing dorsally. Notice that the retrosplenial areas 29 and 30 form the ventral bank of the cingulate gyrus. e) A second dimension flattening was performed in the rostrocaudal direction by selecting the depths of each sulcus (dashed lines in Fig. 1) and moving them rostral or caudal until the depth of the sulcus and/or surface of the cingulate gyrus were represented approximately in the correct distance measured from the one-dimensional flat map and surface photograph. The two-dimensional flat map is shown in Figure 1B. f) The flat map was then copied, reduced to 30% opacity, and the borders of each area identified from histological sections plotted onto the second map (Fig. 1C.). These borders were again adjusted according to findings during high magnification photomicroscopy.

None of the dimensions shown in the flat map can be standardized to coordinates for functional imaging because the two dimensions were highly modified to represent cortex on the surface

and in the posterior cingulate, splenial, and callosal sulci. The macrophotographs of the medial surface of each of the six cases were co-registered to the Talairach and Tournoux coordinate system, the histological border between areas d23b and v23b identified in immunohistochemical sections and on the co-registered medial surfaces and the means±SEM calculated for the distance to the VCA and the bi-commissural lines.

Regional Correlation Analysis in Resting Glucose Metabolism

FDG-PET scanning was performed in 163 drug-free, healthy, right-handed volunteers (age 38 ±18 years, mean±SD; 91 males). FDG-PET data were collected from four centers via on-site advertisements: 68 subjects were scanned at the Cyclotron Research Centre in Liège (Siemens CTI 951 ECAT); 40 at the Department of Nuclear Medicine of the University Hospital Sart Tilman in Liège (Allegro Philips Medical System); 29 at the PET/Biomedical Cyclotron Unit of the Erasmus University Hospital of the Université Libre de Bruxelles in Brussels (Siemens CTI ECAT HR+); and 26 at the Department of Nuclear Medicine of the University Hospital Gasthuisberg of the Katholieke Universiteit Leuven (Siemens CTI ECAT HR+). A separate analysis identifying possible center-related differences in bCCOI did not show significant results for any ROI. A medical doctor (different at each center) excluded subjects with noticeable medical, neurosurgical, neurological or psychiatric history or centrally acting drug intake.

All paid volunteers gave their informed consent and the study was approved by each University's Ethics Committee. They were scanned approximately 15–20 mm above the canthomeatal line in resting conditions with visual and auditory stimulation kept to a minimum. Prior to the acquisition, subjects were instructed to relax, to refrain from moving and to avoid any structured mental activity such as counting, silent singing, etc. Data were reconstructed using a Hanning filter (cutoff frequency: 0.5 cycle/pixel) and corrected for attenuation and background activity. Cerebral metabolic rates for glucose were measured after intravenous injection of 5–10 mCi (185–370 MBq) [^{18}F]fluorodeoxyglucose as described elsewhere (Laureys et al., 2000).

Data were preprocessed and analyzed using statistical parametric mapping (SPM2 version; Wellcome Department of Cognitive Neurology, Institute of Neurology, London, UK; http//www.fil.ion.ucl.ac.uk/spm) implemented in MATLAB (Mathworks Inc., Sherborn, MA). Scans were spatially transformed into a standard stereotactic space and global metabolism normalization was performed by proportional scaling.

Talairach and Tournoux coordinates were converted to MNI coordinates using the tal2mni option, implemented in SPM (written by Matthew Brett; www.mrc-cbu.cam.ac.uk/Imaging/Common/mnispace.shtml; Duncan et al., 2000). Four regions of interest (ROIs) were localized on the canonical Montreal Neurological Institute (MNI) spatially normalized T1 weighted MRI image supplied by SPM2 based on the topography of our histologically identified areas (dPCC, vPCC, area 23d, RSC) using the MRIcro software package (Rorden & Brett, 2000). Mean normalized regional cerebral metabolic rates for glucose within each ROI were used for further functional connectivity assessment (i.e., metabolic cross-correlation studies) as described previously (Laureys et al., 1999). In brief, the entire brain volume was examined for clusters of voxels where metabolic activity correlated significantly with that measured in each of our histologically defined ROIs (dPCC, vPCC, area 23d, RSC). Given that rCMRGlu in area 23d was not independent from that measured in dPCC (high cross-correlation between both ROIs) the former ROI was excluded from further modeling. The other covariates of interest did not show such cross-correlation.

The SPM design matrix included the 163 patients' FDG PET scans (68+40+29+26) and took into account center-related differences in mean levels of glucose consumption. The mean count of FDG uptake of each of the four ROIs served as covariates for interregional correlation analyses, in which voxels showing a significant correlation (i.e., functional connectivity) with the covariate of interest were searched for within the whole brain. Results were considered significant at false discovery rate (FDR)-corrected p value <0.001 (Genovese et al., 2002). In the next step, interaction analyses identified significant differences in functional connectivity between dPCC and vPCC (i.e., regions showing a significant difference in regression slope with dPCC compared to vPCC) (Friston et al., 1997). Results were considered significant at p value <0.001 for the previously identified regions with inclusive making as implemented in SPM2.

Results

Cytological Analysis

Figure 1 orients the medial surface photograph and flat map formats of the posterior cingulate gyrus and sections cut in the coronal plane (i.e., vertical arrow in A). The sulci are also labeled and include a ventral branch (vb; asterisk) of the splenial sulci (spls). This branch is named because it approximates the level of transition between dorsal and ventral divisions of PCC and it is present in most brains. Ono et al. (1990) reported that 84% left and 88% right hemispheres have this branch directed anteriorally toward the corpus callosum. This case was flattened in two dimensions as noted with arrows; dorsally from the dorsal tip of the corpus callosum and in the rostrocaudal direction. The flattening exposes the dorsal and ventral banks of the cingulate gyrus and cortex in the splenial sulci. Using the macro- and microphotographic series, area borders were plotted onto the flat map (outlined with dots in C).

Different magnifications and orientations of histological sections from the gyrus are provided in Figures 2–5. Figure 2 shows the composition of dysgranular area 23d. The essential nature of this cortex is determined by layer IV which is thin and variable. At some points layer IV cannot be distinguished as shown with the "2X" pullout in Figure 2 at a point where neurons in layer IV almost disappear (between the pair of asterisks), although this difference can even be detected at the lower magnification. Figure 2 also provides macrophotographs of the posterior cingulate gyrus through areas d23 (C.) and v23 (B.) and RSC is shown (D.) with a pull out to emphasize its relationship with other areas in the gyrus. The dorsal subicular rudiment (Sub) and indusium griseum (IG) form the fasciolate gyrus dorsal to the corpus callosum and these areas are not part of the ventral bank of the cingulate gyrus. The ectosplenial area 26 is transitional to retrosplenial areas 29 and 30 and is comprised mainly of a single external pyramidal layer, although a few neurons can be seen in the inner pyramidal layer.

Figure 2 shows two anteroposterior levels of area 23; i.e., d23a/b (C.) and v23a/b (B.). These macrophotographs show that area 31 forms the dorsal border of area 23b at all levels. Figure 3 extends the magnification of the area 23b divisions and includes exactly matched SMI32 preparations of neurofilament protein expression (NFP). Comparison with NeuN shows that d23b has less densely packed layer II neurons, smaller pyramids in layer IIIc, a thin layer Va and a relatively sparse layer Vb in comparison to the same layers in v23b. The NFP expressed by large pyramids in both layers IIIc and Vb are more extensive in terms of numbers of labeled neurons in v23b than in d23b. Also, the density of SMI32-labeled pyramids in layer Va in area d23b is sparse in comparison to those in area v23b.

The structures of areas in the cingulate and splenial sulci are shown in Figure 4. Ventral area 24d is shown first for comparative purposes because it is agranular; i.e. lacks a layer IV. Since this area contains the caudal cingulate motor area, it has many large pyramidal neurons in both layers Va and Vb. The arrow pair between low and higher magnification photographs shows

a location for part of the magnified photograph; a box was not placed on the former to avoid obliterating the cytoarchitecture. Notice that no layer IV interdigitates between layers IIIc and Va. Area 23c, in contrast, has a thin layer IV and a very dense layer V (Va in particular). Layer IIIc is also comprised of larger neurons that are more sparse than in area 24d. As a rule, the thickness of layers II–IV in area 23c is significantly greater than the infragranular layers V and VI. Finally, area 31 has a more pronounced layer II, quite large layer IIIc pyramids, a broad layer IV, thick layer Va and a less dense layer Vb than is the case for area 23c. Area 31 has the thickest layer IV of any cingulate area.

To verify the relative differences in cytology in coronal sections, a brain cut in the horizontal plane was analyzed for the PCC dichotomy and differentiation of area 31 as the most caudal extension of the cingulate gyrus. This case is presented at three levels of magnification in Figure 5 where the progressive differentiation of the gyral surface is shown. Since the layer IV/Va borders are aligned in each of the high magnification photographs and lines are drawn through all section, it is possible to view progressive, rostral-to-caudal morphological changes. These include the larger layer IIIc neurons in posterior areas v23b and 31, the particularly wide layer IV in area 31 and the neuron dense layer Vb in both of these areas. Although shown as a progression, there are qualitative differences in the organization of these areas. Most importantly, area 31 shows a shift in the relative size of large deep and superficial neurons with the largest ones in layer IIIc, while the largest ones are in layer Va of area 23. Area v23b has more prominent layers IIIc and IV and more dense neuron packing in layer Vb than does area d23b.

The average location for the border between the dorsal and ventral divisions of area 23 was calculated from all cases after co-registration to Talairach coordinates and the histological location of this border was identified for each co-registered case. The distance from the VCA to the histological border was −5.4±0.17 cm and +1.97±0.08 cm from the bi-commissural line.

Correlation Analysis in Resting Glucose Metabolism

Four ROIs were localized based on the topography of histologically identified areas and regions (dPCC, vPCC, area 23d, RSC). Each ROI subsumed the following areas: dPCC, areas 23d, 23c, d23a/b, 31; vPCC, areas v23a/b, 31; RSC, areas 29 and 30. The ROIs were co-registered to the medial surface coordinates from Talairach and Tournoux and submitted to SPM2 analysis with the MNI standardized space. The histological localization provided an independent means of evaluating basal functional circuitry in a sample of cases of resting glucose metabolism. Although some of the findings are interesting in terms of their topographical relationship to previous reciprocal and monosynaptic projections (Vogt and Pandya, 1987; Cavada and Goldman-Rakic, 1989; Carmichael and Price, 1995; Shibata and Yukie, 2003), they are not necessarily monosynaptic circuits and we refer to correlated clusters of interest in the basal state (bCCOI). Separate analyses identifying possible gender-related differences in bCCOI did not show significant results for any ROI.

Figure 6 provides the glass brain and surface renderings of the bCCOI analysis for three ROIs. The outcome for area 23d is not shown because it is almost the same as that for dPCC; i.e., more than 50% of the dPCC bCCOI are shared with area 23d. The dPCC and vPCC show relatively non-overlapping patterns of correlated activity. For dPCC there is a broad swath on the medial surface including almost all of MCC with the cingulate motor areas in the cingulate sulcus, medial parietal area 7m (precuneus), and the supplementary and pre-supplementary motor areas. A broad swath of correlated voxels is also on the lateral surface and includes inferior parietal cortex and much of superior parietal area 7 and both hemispheres are essentially the same. A similar analysis for area 23d (not shown) had almost the same pattern as for dPCC and this suggests that much of the dPCC correlation analysis is dominated by area 23d.

The bCCOI with vPCC is different in pattern and extent from that of dPCC. Activity on the medial surface is limited to vPCC, ventral area 31, “medial” thalamus, and a small subgenual part of ACC. This latter bCCOI may reflect a monosynaptic connection between the vPCC and ACC (Vogt and Pandya, 1987). Correlated activity on the lateral surface was also quite limited and included caudal temporal and occipital association areas. There was a small correlation on the orbital surface of the left hemisphere and a small one in midtemporal cortex in the same hemisphere. The RSC bCCOI was strikingly limited to the cingulate gyrus and thalamus.

To assess differences in overlap among the various bCCOI, contrasts were performed between dPCC and vPCC as shown in Figure 7. The first analysis (dPCC>vPCC) confirmed the higher functional connectivity of premotor and parietal areas with dPCC as compared to vPCC (A.) parts of parietal cortex and an increase in associated correlations (A.). The second analysis showed a higher modulation of vPCC with subgenual ACC, temporal, occipital and orbitofrontal areas. Thus, the subtractions provide a clear delineation of the patterns of correlated clusters of voxels for each ROI.

Validation of the correlations and graphic demonstration is provided in Figure 8. A voxel in parietal cortex is shown with the cross hairs in two planes of section (−54, −44, 44). This voxel was part of the large cluster of correlated voxels with the dPCC ROI. The graph of these 163 cases shows a significant r of 0.63, while that for vPCC is not significant at 0.15.

To formally test for possible influences of hemisphere-laterality on bCCOI, a separate analysis was performed. The scans were spatially re-normalized using a symmetrical template (Ashburner et al., 1999) and bCCOI obtained for the left hemisphere were compared to those obtained in the flipped right hemisphere as done previously (Laureys et al., 2000). No significant hemisphere-related differences in bCCOI were observed.

Discussion

The dorsal PCC includes areas 23d, d23a/b/c, and adjacent area 31, while ventral PCC includes areas v23a/b and caudal area 31. The cytological analysis shows that area v23 has a more neuron dense layer IV, more neurofilament-expressing layer Va neurons, a dense layer IIIc, and a more dense layer Vb than does area d23. Neither division can be confused with area 31 which has a greater proportion of large layer IIIc pyramids relative to those in layer Va. The dichotomy of PCC based on neuronal architecture confirms that in monkey (Vogt et al., 2005). It is pivotal that each division receives different thalamic afferents because thalamic inputs are associated with the primary functions of an area. Thus, Shibata and Yukie (2003) showed that d23 has unique inputs from the mediodorsal, central latocellular, and ventral anterior and lateral nuclei. Structural differentiation of PCC provides a powerful approach to guide defining ROIs in an FDG-PET study that showed very different bCCOI for each PCC division. This finding provides the basis for a new analysis of the functional imaging literature and, as discussed below, the outcome of this analysis supports the expectation that each subregion is involved in fundamentally different aspects of information processing; the vPCC in self-reflection via engagements with subgenual ACC and the dPCC in visuospatial and body orientation via interactions with numerous premotor areas including the cingulate motor areas.

Overview of Posteromedial Cingulate Function

Before considering the functions and connections of the dPCC and vPCC separately, it is instructive to note imaging tasks that activate medial parietal cortex (precuneal area 7m), PCC and RSC together; hence the function of this entire region. Burgess et al. (2001) used the virtual reality of a complex town setting as a context for real world presentation of events, people, and objects. Since subjects were scanned during retrieval, a memory component was also engaged. Contrast of place with non-memory conditions activated a swath of medial cortex including

precuneal area 7m, PCC, RSC, and posterior hippocampal and parahippocampal cortices. Thus, many aspects of personal, spatial recognition and context, objects, and memory are triggered during this task and these areas operate simultaneously under these conditions.

The PCC and RSC have long been recognized to be involved in memory access and topographic orientation in human ablation (Valenstein et al., 1987), stroke (Takahashi et al., 1997; Maguire, 2001), and imaging (Maguire et al., 1999; Maguire, 2001; Piefke et al., 2003) studies. The topokinetic memory network includes parietal, insular, cingulate and hippocampal cortices (Berthoz, 1999). Neurons in area 23 of PCC code for the orbital position of the eye and respond to large textured visual fields (Olson et al., 1993, 1996). This information together contributed to the rationale for a four-region neurobiological model of the primate cingulate gyrus which postulates the essential function of the PCC as subserving visuospatial orientation (Vogt et al., 2004). The present question is not the overall function of this region or any one area, but rather, to what extent can each component of these complex tasks be attributed to a unique structure/function entity in the posterior cingulate gyrus and can the dorsal and ventral divisions of area 23 be functionally differentiated?

Functional Considerations: vPCC in Ongoing Self Monitoring

The four-region neurobiological model of cingulate cortex postulates that the ACC is involved in autonomic driving and emotional memory, however, PCC also responds to emotional scripts and faces even though it does not have direct autonomic connections (Neafsey et al., 1993; George et al., 1995, 1996; Mayberg et al., 1999; Vogt et al., 2003, 2004). Is the emotional driving of ACC and PCC equivalent? The important fact is that, although PCC is active during simple emotions driven by faces or scripts, it is also activated by non-emotional scripts or faces (Fink et al., 1996; Maguire and Mummery, 1999; Shah et al., 2001; Bernstein et al., 2002) as shown in Figure 9 and excerpted from Vogt et al. (2003). In contrast, ACC is not active during non-emotional face and script evaluation. Thus, the role of vPCC in emotion is different from that of ACC and a hypothesis is needed that integrates current functional imaging and connection information. The bCCOI study of vPCC showed a high level of correlated activity in subgenual ACC and is interesting in terms of the reciprocal and monosynaptic connection previously identified with anatomical techniques in monkey (Vogt and Pandya, 1987). We propose that vPCC evaluates all information arriving through the ventral visual stream as discussed below and this provides for an information flow that is continually assessed for the emotional consequences of visual events and the emotional content is determined from information stored in subgenual ACC. Thus, the vPCC is not part of an emotion system *per se*, but provides the code for relevant information from visual sensory systems to evaluate emotional content.

In addition to simple emotions, studies involving self reflection also activate vPCC. Johnson et al. (2002) used such a task and the boundary of their activated region is outlined with black dots in Figure 9 (self reflection). The activation includes much but not all of vPCC and has only a small extension into dPCC. Other studies of one's own face (Kircher et al., 2001; Sugiura et al., 2005), familiar faces (Maddock et al., 2001), and intentional self assessment (Kircher et al., 2002) activate a similar region shown in the pull out in Figure 9B. A study by Denton et al. (1999) demonstrated thirst activation in ACC; however, when brain activation was correlated with the thirst score, a robust activation was shown posterior to the splenium of the corpus callosum in vPCC. At first a thirst correlation may seem contradictory to the proposed function for this region; however, if viewed as an assessment of internal state and for self-relevance, this finding is compatible with the proposed function.

Not all studies meet our expectations for self-reflective function of vPCC. A third-person reflection activated dPCC and vPCC, while the first person failed to activate vPCC (Ruby and

Decety, 2001). It is possible that the references were too general and not subject-selective in this study. Another study that may at first appear to be at odds with our conclusion is a study of self-referential trait adjectives which showed an increase in ACC and a decrease in dPCC (Kelley et al., 2002). This latter study, however, more likely engaged word selection processes much as the verb generation task of Raichle et al. (1994) rather than an internal self-evaluative state. The brain pattern of activation and inactivation sites supports its similarity to word generation tasks (Raichle, 2000). Finally, Uddin et al. (2005) observed a higher level of activation in vPCC while subjects assessed other faces than their own faces. It is possible that differences among the stimuli were more subtle than in previous studies or we do not yet fully understand processing of facial information in this region.

We propose that the vPCC is at an intermediate stage of information processing between visual recognition in visual cortex and emotion-related substrate in sACC. In vPCC emotional objects and past events are evaluated among many inputs for self relevance. In keeping with this view, sensory facial recognition processing occurs on the fusiform gyrus before assessments of emotional content in the cingulate gyrus (Grill-Spector et al., 2004). Emotional assessment of objects and events first requires differentiation of potentially emotional objects/events from non-emotional ones. Since valences are assigned in ACC, this region stores those memories (George et al., 1995, 1996; Mayberg et al., 1999), regulates autonomic activity associated with emotion (Neafsey et al., 1993), and no non-emotion activity drives ACC (Vogt et al., 2003), the reciprocal connection between vPCC and ACC is very important to these processes. The hypothesis for vPCC function suggests that it selects among emotion and non-emotion events and assesses self relevance via interactions with ACC.

Functional Considerations: dPCC in Self Orientation in Visual Space

The dPCC may not be involved in emotion and non-emotion script and face processing (Fig. 9; Vogt et al., 2003) and it is this dorsal region of PCC in the monkey that contains neurons responsive to the orbital position of the eye and large and textured visual field stimulation (Olson et al., 1993,1996). Four studies plotted in the Figure 9 pull out report changes in this region associated with visual feedback of moving hands (Inoue et al., 1998), predictability of self-generated actions (Blakemore et al., 1997), free exploration in a virtual reality maze (Maguire et al., 1998), and complex London route recall (Maguire et al., 1997). Thus, the role of dPCC is in orientation of self and body in visual space.

Circuitry Analysis

Dorsal and ventral PCC differentiation and visual streams

In addition to differences in thalamic afferents to the monkey dorsal and ventral PCC observed by Shibata and Yukie (2003), our bCCOI study in human shows a radical difference in correlated voxels associated with the dPCC and vPCC and these differences reflect the functional organization discussed above. Since approximately 50% of the bCCOI associated with dPCC are also correlated with area 23d, the pattern and density of bCCOI with this area was similar to that of dPCC. The most striking finding is that inputs to the two PCC divisions are associated with the dorsal and ventral visual pathways as originally described by Ungerleider and Mishkin (1982). They viewed the dorsal pathway as involved in spatial processing, while the ventral pathway was mainly involved in object processing. Figure 10 takes the lateral surfaces from the bCCOI studies and aligns them in the context of the dorsal and ventral visual pathways. There is a major association of dPCC and area 23d with posterior parietal cortex as is also known from monosynaptic monkey connection studies (Vogt and Pandya, 1987; Cavada and Goldman-Rakic, 1989). This circuit is maintained via intracingulate processing such that bCCOI extend through most of MCC, including the cingulate motor areas in the sulcus and supplementary/pre-supplementary motor cortices.

The vPCC receives a massive input from the superior and middle temporal gyri in keeping with projections of the ventral visual stream. In contrast to dPCC, the vPCC has only minimal interactions with cingulate cortex and this is with subgenual ACC. As noted above, this region is specifically involved in emotion because it stores emotional memories and drives autonomic activity (Vogt et al., 2003). Processing in the vPCC/ACC circuit is enhanced via connections through medial orbitofrontal cortex (mOFC). Although both the dorsal and ventral divisions of PCC have a significant aggregate of bCCOI in mOFC, those with vPCC are shown in Figure 10 because of findings in monkey cortex. Carmichael and Price (1995; their Fig. 15) showed that both perigenual area 24 and vPCC are connected with area 11m and suggest an important site at which the combined activities in both cingulate areas interact in medial orbital cortex. Thus, coordination of self assessments in vPCC with emotional memories in ACC and relevant autonomic changes may occur in mOFC.

Motor access via the cingulate motor areas

The extensive bCCOI throughout MCC associated with the dPCC included the cingulate motor areas and suggest a pivotal and direct linkage to motor output via the dPCC that is not shared by the vPCC. Indeed, one of the criteria for identifying the midcingulate region is that it regulates skeletomotor functions through two cingulate motor areas (CMA); one in anterior MCC (rostral CMA-rCMA) and one in posterior MCC (caudal CMA-cCMA; reviewed in Vogt et al., 2003, 2004). There is almost no evidence for a role in simple emotions or autonomic functions for pMCC or dPCC (Vogt et al., 2003; Vogt, 2005) and nociceptive evoked potentials demonstrate activity in this region which may be associated with movement outside the context of pain. Bentley et al. (2003) showed that noxious thermal stimulation to the hand activated sites in areas p24′, d23, and 23d. Niddam et al. (2005) applied noxious and innocuous electrical stimulation to a finger muscle and activated two cingulate sites; one in area 24d where the cCMA is located and one in area 23d. Furthermore, electrical stimulation of dPCC in epileptic subjects evoked complex proprioceptive sensations (Richer et al., 1993) and the motor relevance of this region was made explicit by Huang et al. (2004) who used magnetoencephalography to evaluate movement-associated activity during self-paced, finger lifting movements and showed a site in area 23d. Thus, activity in areas p24′ and 23d is associated with direct access to the cCMA (Vogt, 2005) and this provides the final link in circuitry for differential outputs from the dPCC that may arise in the dorsal visual stream.

There are likely indirect circuits by which vPCC and mOFC access the CMAs and the consequences of their interactions with subgenual ACC may lead to outputs from the CMAs. Notice that mOFC has substantial bCCOI with dPCC and mOFC has reciprocal connections with the ventral parts of both dPCC and vPCC (Carmichael and Price, 1995) and neurons between the orbital sulci project to MCC (Vogt and Pandya, 1987). Processing in the vPCC/ACC circuit is enhanced via connections through mOFC as shown in Figure 10 and, compared to the dPCC, the vPCC has a more significant aggregate of bCCOI in mOFC (Fig. 7B). These findings are in line with those in monkey cited above. Thus, the loop to motor output from the vPCC/ACC interaction in mOFC may be completed by projections from mOFC to dPCC (dashed line/arrow in Fig. 10) and from there into premotor circuits. The dPCC, therefore, has direct projections to CMAs, while that from the vPCC is indirect and possibly co-modulated with mOFC projections.

Retrosplenial Cortex

The RSC is adjacent to dPCC and vPCC, it has reciprocal connections with area d23a (Vogt and Pandya, 1987; Morris et al., 1999), and it participates in memory associated with the functions of dPCC. For example, tasks requiring memory of routes learned from the environment (Ghaem et al., 1997; Mellet et al., 2000) activate RSC and lesions, strokes, or tumors in this region produce amnesia including topokinetic disorientation (Valenstein et al.,

1987; Rudge and Warrington, 1991; Takahashi et al., 1997). In view of the direct connections between RSC and dPCC and participation in common functions, the bCCOI analysis showed a restricted cingulate gyrus pattern of correlated voxels most prominently located in the posterior MCC and PCC, although there was an additional extension along the rostrum of the corpus callosum. To the extent that bCCOI might demonstrate functional circuits, the RSC has a restricted interaction throughout the cingulate gyrus. In spite of the heavy and monosynaptic connections of RSC with parahippocampal cortex in the monkey (Vogt and Pandya, 1987), no bCCOI were observed in this latter gyrus and it is unclear what this dissociation indicates about the interactions of dPCC and parahippocampal areas in RSC. Although these observations provide a striking mismatch between expected functional interactions based on monosynaptic connections and bCCOI analysis, one reason for the apparent mismatch could be technical in nature as discussed below.

Retrosplenial cortex is comprised of areas 29 and 30 and these areas are located on the ventral bank of the cingulate gyrus in the callosal sulcus and form transitional structures between the allocortical area 26 and isocortical area 23a (Braak, 1979; Vogt et al., 2001; Zilles, 2004). Although Brodmann placed RSC on the caudomedial lobule, he was using a convoluted brain to plot the areas. Since about 50% of PCC is in the callosal, cingulate, and splenial sulci, it was not possible for him to accurately show the topographical limits of cortical areas in sulci without flattening. His placing RSC on the surface of the caudomedial lobule instead of in the callosal sulcus, led to the incorrect extrapolation by Talairach and Tournoux (1988) and other standardized atlases of RSC to the surface of the posterior cingulate gyrus and the result is a conflicting body of work about the functions of areas 23/31 and 29/30 (Vogt et al., 2000, 2001). Designation of cingulate areas at x= +/− 14 and y= −50 to −60 as RSC continues because atlases refer to this as area 30 in parasagittal sections and in coronal sections at y= −55 to −60 it is labeled area 31. This cortex is comprised of areas v23a/b and v31 but not RSC.

Methodological Issues

An unavoidable limitation in our histological and metabolic study is that the histological investigations were not and cannot be done in the same individuals as our *in vivo* metabolic measurements. In part, this limitation was compensated for by the comparatively large number of individuals investigated (6 histological; 163 metabolic). It is also important to stress that the spatial resolution of PET imaging is low compared to the histological assessments. To enhance anatomical localization, the PET data ideally should have been coregistered with MRI data for each individual. Given that we did not possess the MRI data for all 163 individuals, this could not be done. Although the results should be interpreted with caution, it is unlikely to alter the relevance of our results given their high degree of significance when comparing vPCC and dPCC differences in bCCOI.

Another restricting factor in the functional interpretation of the bCCOI analyses is that the PET data were acquired during the so-called “resting state” (Gusnard and Raichle, 2001; Mazoyer et al., 2001; Greicius et al., 2003). Since this “resting state” is not free of cognitive activity, analysis of various challenge conditions according to the dPCC/vPCC dichotomy should provide further insight into functional connectivity in both health and disease.

One of the dilemmas raised by the present findings is the lack of a substantial bCCOI to support a connection between RSC and PCC reported previously in monkey (Vogt and Pandya, 1987; Morris et al., 1999). One possibility is that the interaction between these regions is not easily engaged because they have resting states that are very different. Alternatively, this results from the method itself. Defining the RSC ROI in the depths of the callosal sulcus requires precision that may be at the limits of the coregistration approach for FDG-PET and there may be substantial and extraneous white matter in the ROI. In this latter situation, it could be that

a disproportionately high level of grey to white matter identifies bCCOI that do not actually reflect resting CMRglu in the RSC and this could be misleading when evaluating the entire cingulate gyrus and cerebral cortex.

Diffusion tensor imaging has become a popular means of analyzed white matter and it is sometimes misconceived of as a tool for studying connections. Although it provides insight into white matter architecture, it cannot show specific connections because it cannot track connections from their origin in the gray matter to their termination sites in the gray matter. Theoretically, it is impossible to tract single axons from their origin in a pyramidal neuron axon hillock to its terminal field. Indeed, many "connections" that have been reported have never been observed in monkey connection studies; i.e., they represent false positives. For example, Guye et al. (2003) make excellent use of diffusion tensor imaging by coupling it with a fast-marching tractography algorithm. Although this approach generated many connections of primary motor cortex that can be supported from the literature, others simply do not exist and include the following: middle cerebellar peduncle, occipital lobe, fornix, corpus callosum (the distal limbs have no callosal connections), and posterior cingulate gyrus.

Concerns about diffusion tensor imaging can be similarly raised with the bCCOI method in terms of false positive and false negative "connections." The underlying assumption for the present method is that areas with common resting levels of metabolism are more likely to interchange information as the circuit is functionally engaged. There have been some surprising supporting findings of established connections (vPCC and ACC; dPCC and mOFC; differentiation of visual and parietal input to divisions of PCC). Indeed, the importance of mOFC was not appreciated until these studies were completed. Although these connections have counterparts in the monkey as discussed above, there are also outstanding mismatches between predicted and observed results as also noted for RSC. Another mismatch is that, although parietal projections to cingulate cortex are substantial (Vogt and Pandya, 1987; Cavada and Goldman-Rakic, 1989), they are not nearly as broad as the bCCOI analyses suggest. This may be viewed as a false positive but this in itself is of some interest. The PCC may have a much greater access to parietal lobe output than suggested by neuroanatomical studies. Although area LIP, for example, is a gateway by which parietal information reaches the cingulate gyrus, activity in a much wider parietal region may influence cingulate functions than previously thought. Thus, bCCOI analyses and diffusion tensor imaging do not provide a precise and equivalent mapping of monosynaptic connections that can be achieved in monkey cortex; however, even the fact that some of these connections can be identified is a rather amazing and this provides a basis for studying further the functions of these circuits and their reorganization in disease states.

The Future for Circuitry Analysis of Human Cingulate Cortex

The current results suggest many avenues for future development. Quantitative probability maps of the areas on the cingulate gyrus would be useful in making modern maps of the cingulate gyrus available to the general imaging research community. The need for maps based on histological reality rather than poor extrapolations from Brodmann without histological verification has been noted in the present study for RSC but similar comments are justified for many areas in the cingulate gyrus including the subdivisions of MCC and ACC. The cytoarchitectural complexion of the primate cingulate gyrus has changed radically from the time of Brodmann. Probabilistic maps have proved useful for somatosensory cortex (Grefkes et al., 2001) and Eichhoff et al. (2005) discuss a method for evaluating area localization using SPM.

One of the most important advances will derive from evaluating the flow of information in these networks and from assessing changes in connectivity during functional challenges. The

most obvious undertaking will be to demonstrate the functional dichotomy of inputs to PCC from the two visual systems. A recent report of the “what” and “where” processing streams for tactile stimuli showed that MCC was primarily activated during tactile object recognition (Reed et al., 2005). Similar studies would be most interesting to test hypotheses about differential processing of visual information in similar pathways to vPCC and dPCC.

Linking the topography of transmitter systems with the dPCC and vPCC subregions will provide important new information about circuitry and function that could lead to new avenues of drug therapeutics. Direct linking of cytoarchitectural and receptor binding findings with multivariate modeling has been demonstrated for human parietal cortex (Zilles and Palomero-Gallagher, 2001) and its application to the cingulate gyrus in the monkey demonstrated (Bozkurt et al., 2005). Now that the PCC dichotomy has been uncovered along with its circuitry in human and monkey brains, we are certain to move closer to the underlying contributions of the posterior cingulate gyrus to human behavior.

Acknowledgements

This work was supported by the National Institutes of Health (NINDS grant #044222; BAV) and the Fonds National de Recherche Scientifique (SL). We thank Pierre Maquet, Eric Salmon, Gaetan Garroux and André Luxen (Cyclotron Research Centre, Liège); Roland Hustinx (Department of Nuclear Medicine, University Hospital Sart Tilman, Liège); Serge Goldman, Xavier De Tiège, and Patrick Van Bogaert (PET/Biomedical Cyclotron Unit, Erasmus University Hospital, Brussels) and Koen Van Laere (Department of Nuclear Medicine, University Hosptial of Gasthuisberg, Leuven) for kindly sharing the PET data.

Abbreviations

ACC
: anterior cingulate cortex (equivalent to perigenual cortex; pACC)

bCCOI
: basal correlated clusters of interest

cas
: callosal sulcus

cc
: corpus callosum

cgs
: cingulate sulcus

CMA; c; r
: cingulate motor area; rostral and caudal

CMRGlu
: cerebral metabolic rate for glucose

dPCC
: dorsal division of PCC

FDG
: [^{18}F] flurodeoxyglucose

IG
: indusium griseum

MCC

midcingulate cortex

mOFC
medial orbitofrontal cortex

mr
marginal ramus

NFP
neurofilament proteins

PBS
phosphate buffered saline

PET
positron emission tomography

PCC
posterior cingulate cortex

pMCC
posterior midcingulate cortex

Pos
parieto-occipital sulcus

RSC
retrosplenial cortex

SEM
standard error of the mean

SMI32
antibody to intermediate neurofilament proteins

Spls
splenial sulci

Sub
dorsal subiculum

vb
ventral branch of the splenial sulci

VCA
vertical plane at the anterior commissure

vPCC
ventral division of PCC

References

Ashburner J, Andersson JL, Friston KJ. High-dimentional image registration using symmetric priors. NeuroImage 1999;9:619–628. [PubMed: 10334905]

Bentley DE, Derbyshire SWG, Youell PD, Jones AKP. Caudal cingulate cortex involvement in pain processing: an inter-individual laser evoked potential source localization study using realistic head models. Pain 2003;102:265–271. [PubMed: 12670668]

Bernstein LJ, Beig S, Siegenthaler AL, Grady CL. The effect of encoding strategy on the neural correlates of memory for faces. Neuropsychologia 2002;40:86–89. [PubMed: 11595264]

Berthoz A. Parietal and hippocampal contribution to topokinetic and topographic memory. Phil Trans Royal Soc Lond Series B: Biolog Sci 1997;352:1437–1448.

Berthoz, A. Hippocampal and parietal contribution to topokinetic and topographic memory. In: Burgess, N.; Jeffery, KJ.; O'Keefe, J., editors. The Hippocampal and Parietal Foundations of Spatial Cognition. Oxford University Press; Oxford: 1999.

Blakemore SJ, Rees G, Frith CD. How do we predict the consequences of our actions? A functional imaging study. Neuropychologia 1998;36:521–529.

Bottini G, Cappa S, Geminiani G, Sterzi R. Topographic disorientation- A case report. Neuropsychologia 1990;28:309–312. [PubMed: 2325843]

Braak H. Pigment architecture of the human Telencephalic cortex. IV. Regio retrosplenialis. Cell Tiss Res 1979;204:431–440.

Bozkurt A, Zilles K, Schleicher A, Kamper L, Arigita ES, Uylings BM, Kötter R. Distributions of transmitter receptors in the macaque cingulate cortex. NeuroImage 2005;25:219–229. [PubMed: 15734357]

Brodmann, K. Vergleichende Localisationslehre der Grosshirnrinde in Ihren Prinzipien Dargestellt auf Grund des Zellenbaues. J.A. Barth; Leipzig: 1909.

Burgess N, Maguire EA, Spiers HJ, O'Keefe J. A temporoparietal and prefrontal network for retriving the spatial context of lifelike events. NeuroImage 2001;14:439–453. [PubMed: 11467917]

Carmichael ST, Price JT. Limbic connections of the orbital and medial prefrontal cortex in macaque monkeys. J Comp Neurol 1995;363:615–641. [PubMed: 8847421]

Cavada C, Goldman-Rakic PS. Posterior parietal cortex in rhesus monkey: I. Parcellation of areas based on distinctive limbic and sensory corticocortical connections. J Comp Neurol 1989;287:393–421. [PubMed: 2477405]

Damasio AR, Grabowski TJ, Bechara A, Damasio H, Ponto LL, Parvizi J, Hichwa RD. Subcortical and cortical brain activity during the feeling of self-generated emotions. Nature Neurosci 2000;3:1049–1056. [PubMed: 11017179]

Denton D, Shade R, Zamanppa F, Eagan G, Blair-West J, McKinley M, Lancaster J, Fox P. Neuroimaging of genesis and satiation of thirst and an interoceptor-driven theory of origins of primary consciousness. Proc Natl Acad Sci, USA 1999;96:5304–5309. [PubMed: 10220461]

Duncan J, Seitz RJ, Kolodny J, Bor D, Herzog H, Ahmed A, Newell FN, Emslie H. A neural basis for general intelligence. Science 2000;289:457–560. [PubMed: 10903207]

Eickhoff SB, Stephanm KE, Mohlberg H, Grefkes C, Fink GR, Amunts K, Zilles K. A new SPM toolbozx for combining probabilistic cytoarchitectonic maps and functional imaging data. NeuroImage 2005;25:1325–1335. [PubMed: 15850749]

Fink GR, Markowitsch HJ, Reinkemeier M, Bruckbauer T, Kessler J, Heiss WD. Cerebral representation of one's own past: neural networks involved in autobiographical memory. J Neurosci 1996;16:4275–4282. [PubMed: 8753888]

Friston KJ, Buechel C, Fink GR, Morris J, Rolls E, Dolan RJ. Psychophysiological and modulatory interactions in neuroimaging. NeuroImage 1997;6:218–229. [PubMed: 9344826]

Genovese CR, Lazar NA, Nichols T. Thresholding of statistical maps in functional neuroimaging using the false discovery rate. NeuroImage 2002;15:870–878. [PubMed: 11906227]

George MS, Ketter TA, Parekh PI, Herscovitch P, Post RM. Gender differences in regional cerebral blood flow during transient self-induced sadness or happiness. Biolog Psychiatry 1996;40:859–871.

George MS, Ketter TA, Parekh PI, Horwitz B, Herscovitch P, Post RM. Brain activity during transient sadness and happiness in healthy women. Am J Psychiatry 1995;152:341–351. [PubMed: 7864258]

Ghaem O, Mellet E, Crivello F, Tzourio N, Mazoyer B, Berthoz A, Denis M. Mental navigation along memorized routes activates the hippocampus, precuneus, and insula. NeuroReport 1997;8:739–744. [PubMed: 9106758]

Grefkes C, Geyer S, Schorrman T, Roland P, Zilles K. Human somatosensory area 2: observer-independent cytoarchite3ctonic mapping, interindividual variability, and population map. NeuroImage 2001;14:617–631. [PubMed: 11506535]

Greicius MD, Krasnow B, Reiss AL, Menon V. Functional connectivity in the resting brain: a network analysis of the default mode hypothesis. Proc Natl Acad Sci USA 2003;100:253–258. [PubMed: 12506194]

Grill-Spector K, Knouf N, Kanwisher N. The fusiform face area subserves face perception, not generic within-category identification. Nature Neurosci 2004;7:555–568. [PubMed: 15077112]

Guye M, Parker JM, Symms M, Boulby P, Wheeler-Kingshott CAM, Salek-Haddadi A, Barker GJ, Duncan JS. Combined functional MRI and tractography to demonstrate the connectivity of the human primary motor cortex in vivo. NeuroImage 2003;19:1349–1360. [PubMed: 12948693]

Huang M-X, Harrington DL, Paulson KM, Weisend MP, Lee RR. Temporal dynamics of ipsilateral and contralateral motor activity during voluntary finger movement. Human Brain Mapping 2004;23:26–39. [PubMed: 15281139]

Inoue K, Kawashima R, Satoh K, Kinomura S, Goto R, Koyama M, Sugiura M, Ito M, Fukuda H. PET study of pointing with visual feedback of moving hands. J Neurophysiol 1998;79:117–125. [PubMed: 9425182]

Johnson SC, Baxter LC, Wilder LS, Pipe JG, Heiserman JE, Prigatano GP. Neural correlates of self-reflection. Brain 2002;125:1808–1814. [PubMed: 12135971]

Kelley WM, Macrae CN, Wyland CL, Caglar S, Inati S, Heatherton TF. Finding the self? An event-related fMRI study. J Cog Neurosci 2002;14:785–794.

Kircher TTJ, Brammer M, Bullmore E, Simmons A, Bartels M, David AS. The neural correlates of intentional and incidental self processing. Neuropsychologia 2002;40:683–692. [PubMed: 11792407]

Kircher TTJ, Senior C, Phillips ML, Rabe-Hesketh S, Benson PJ, Bullmore ET, Brammer M, Simmons A, Bartels M, David AS. Recognizing one's own face. Cognition 2001;78:B1–B15. [PubMed: 11062324]

Laureys S, Faymonville ME, Degueldre C, Del Fiore G, Damas P, Lambermont B, Janssens N, Aerts J, Franck G, Luxen A, Moonen G, Lamy M, Maquet P. Auditory processing in the vegetative state. Brain 2000;123:1589–1601. [PubMed: 10908189]

Laureys S, Goldman S, Phillips C, Van Bogaert P, Aerts J, Luxen A. Impaired effective cortical connectivity in vegetative state: preliminary investigation using PET. NeuroImage 1999;9:377–382. [PubMed: 10191166]

Maddock RJ, Garrett AS, Buonocore MH. Remembering familiar people: The posterior cingulate cortex and autobiographical memory retrieval. Neuroscience 2001;104:667–676. [PubMed: 11440800]

Maguire EA. The retrosplenial contribution to human navigation: A review of lesion and neuroimaging findings. Scand J Psychol 2001;42:225–238. [PubMed: 11501737]

Maguire EA, Frackowiak RSJ, Frith CD. Recalling routes around London: Activation of the right hippocampus in taxi drivers. J Neurosci 1997;17:7103–7110. [PubMed: 9278544]

Maguire EA, Frith CD, Burgiss N, Donnett JG, O'Keefe J. Knowing where things are: parahippocampal involvement in encoding object locations in virtual large-scale space. J Cog Neurosci 1998;10:61–76.

Maguire EA, Frith CD, Morris RGM. The functional neuroanatomy of comprehension and memory: the importance of prior knowledge. Brain 1999;122:1839–1850. [PubMed: 10506087]

Maguire EA, Mummery CJ. Differential modulation of a common memory retrieval network revealed by positron emission tomography. Hippocampus 1999;9:54–61. [PubMed: 10088900]

Mayberg HS, Liotti M, nan SK, McGinnis S, Mahurin RK, Jerabek JA, Tekell JL, Martin CC, Lancaster JL, Fox PT. Reciprocal limbic-cortical function and negative mood; converging findings in depression and normal sadness. Am J Psychiatry 1999;156:675–682. [PubMed: 10327898]

Mellet E, Bricogne S, Tzourio-Mazoyer N, Ghaem O, Petit L, Zago L, Etard O, Berthoz A, Mazoyer B, Denis M. Neural correlates of topographic mental exploration: the impact of route versus survey perspective learning. NeuroImage 2000;12:588–600. [PubMed: 11034866]

Morris R, Petrides M, Pandya DN. Architecture and connections of retrosplenial area 30 in the rhesus monkey (Macaca mulatta). Eur J Neurosci 1999;11:2506–2518. [PubMed: 10383640]

Neafsey, EJ.; Terreberry, RR.; Hurley, KM.; Ruit, KG.; Frysztak, RJ. Anterior cingulate cortex in rodents: Connections, visceral control functions, and implications for emotion. In: Vogt, BA.; Gabriel, M.,

editors. Neurobiology of Cingulate Cortex and Limbic Thalamus. Birkhäuser; Boston: 1993. p. 207-223.

Niddam DM, Chen LF, Wu YT, Hsieh JC. Spatiotemporal brain dynamics in response to muscle stimulation. NeuroImage 2005;25:942–951. [PubMed: 15808994]

Olson, CR.; Musil, SY.; Goldberg, ME. Posterior cingulate cortrex and visuospatial cognition: Properties of single neurons in the behaving monkey. In: Vogt, BA.; Gabriel, M., editors. Neurobiology of Cingulate Cortex and Limbic Thalamus. Birkhäuser; Boston: 1993.

Olson CR, Musil SY, Goldberg ME. Single neurons in posterior cingulate cortex of behaving macaque: Eye movement signals. J Neurophysiol 1996;76:3285–3300. [PubMed: 8930273]

Ono, M.; Kubik, S.; Abernathey, CD. Atlas of the Cerebral Sulci. Georg Thieme Verlag; Stuttgart and New York: 1990.

Parker A, Gaffan D. The effect of anterior thalamic and cingulate cortex lesions on object-in-place memory in monkeys. Neuropsychologia 1997;35:1093–1102. [PubMed: 9256374]

Phan KL, Ho S-H, Taylor SF, Welsh RC, Britton JC, Liberzon I. Dissociable neural responses during appraisal of emotional stimuli: An fMRI study. Soc Neurosci Abs. 2003Program No. 725.3

Phan KL, Wager T, Taylor SF, Liberzon I. Functional neuroanatomy of emotion: a meta-analysis of emotion activation studies in PET and fMRI. NeuroImage 2002;16:331–348. [PubMed: 12030820]

Phillips ML, Bullmore ET, Howard R, Woodruff PWR, Wright IC, Williams SCR, Simmons A, Andrew C, Brammer M, David AS. Investigation of facial recognition memory and happy and sad facial expression perception: an fMRI study. Psychiatry Res Neuroimaging Section 1998;83:127–138.

Piefke M, Weiss PH, Zilles K, Markowitch HJ, Fink GR. Differential remotenss and emotional tone modulate the neural correlates of autobiographical memory. Brain 2003;126:650–668. [PubMed: 12566286]

Raichle ME, Fiez JA, Videen TO, MacLeod AK, Pardo JV, Fox PT, Petersen SE. Practice-related changes in human brain functional anatomy during nonmotor learning. Cerebral Cortex 1994;4:8–26. [PubMed: 8180494]

Raichle, ME. The neural correlates of consciousness: An analysis of cognitive skill learning. In: Gazzaniga, MS., editor. The New Cognitive Neurosciences. MIT Press; Cambridge, MA: 2000. p. 1305-1318.

Reed CL, Klatzky RL, Halgren E. What vs where in touch: an fMRI study. NeuroImage 2005;25:718–726. [PubMed: 15808973]

Richer F, Martinez M, Robert M, Bouvier G, Saint-Hilaire J-M. Stimulation of human somatosensory cortex: tactile and body displacement perceptions in medial regions. Exper Brain Res 1993;93:173–176. [PubMed: 8467887]

Rorden C, Brett M. Stereotaxic display of brain lesions. Behav Neurol 2000;12:191–200. [PubMed: 11568431]

Ruby P, Decety J. Effect of subjective perspective taking during simulation of action: a PET investigation of agency. Nature Neurosci 2001;4:546–550. [PubMed: 11319565]

Rudge P, Warrington EK. Selective impairment of memory and visual perception in splenial tumors. Brain 1991;114:349–360. [PubMed: 2004246]

Shah NJ, Marshall JC, Zafiris O, Schwab A, Zilles K, Markowitsch HJ, Fink GR. The neural correlates of person familiarity: a functional magnetic resonance imaging study with clinical implications. Brain 2001;124:804–15. [PubMed: 11287379]

Shibata H, Yukie M. Differential thalamic conncections of the posteroventral and dorsal posterior cingulate gyrus in the monkey. Eur J Neurosci 2003;18:1615–1626. [PubMed: 14511340]

Sugiura M, Watanabe J, Maeda Y, Matsue Y, Fukuda H, Kawashima R. Cortical mechanisms of visual self-recognition. NeuroImage 2005;24:143–149. [PubMed: 15588605]

Takahashi N, Kawamura M, Shiota J, Kasahata N, Hirayama K. Pure topographic disorientation due to right retrosplenial lesion. Neurology 1997;49:464–469. [PubMed: 9270578]

Talairach, J.; Tournoux, P. Co-planar stereotaxic atlas of the human brain. Theime Medical Publishers; New York: 1988.

Uddin LQ, Kaplan JT, Molnar-Szakacs I, Zaidel E, Iacoboni M. Self-face recognition activates a frontoparietal “mirror” network in the right hemisphere: an event-related fMRI study. Neuroimage 2005;25:926–935. [PubMed: 15808992]

Ungerleider, LG.; Mishkin, M. Two cortical visual systems. In: Ingle, DJ.; Mansfield, RJW., editors. Analysis of Visual Behavior. Cambridge, MA: MIT Press; 1982. p. 549-586.

Valenstein E, Bowers D, Verfaellie M, Heilman KM, Dayh A, Watson RT. Retrosplenial amnesia. Brain 1987;110:1631–1646. [PubMed: 3427404]

Vogt BA. Pain and emotion interactions in subregions of the cingulate gyrus. Nat Rev Neurosci 2005;6:533–545. [PubMed: 15995724]

Vogt BA, Berger GR, Derbyshire SWG. Structural and functional dichotomy of human midcingulate cortex. Eur J Neurosci 2003;18:3134–3144. [PubMed: 14656310]

Vogt BA, Bush G, Absher JR. Human retrosplenial cortex: Where is it and is it involved in emotion? Trends Neurosci 2000;23:195–196. [PubMed: 10782121]

Vogt BA, Pandya DN. Cingulate cortex of the rhesus monkey. II. Cortical afferents. J Comp Neurol 1987;262:271–289. [PubMed: 3624555]

Vogt, BA.; Hof, PR.; Vogt, L. Cingulate gyrus. In: Paxinos; Mai, JK., editors. The Human Nervous System. Vol. 2. Elsevier; San Diego: 2004. p. 915-949.

Vogt BA, Vogt L, Farber NB, Bush G. Architecture and neurocytology of the monkey cingulate gyrus. J Comp Neurol 2005;485:218–239. [PubMed: 15791645]

Vogt BA, Vogt LJ, Perl DP, Hof PR. Cytology of human caudomedial cingulate, retrosplenial, and caudal parahippocampal cortices. J Comp Neurol 2001;438:353–376. [PubMed: 11550177]

Zilles, K. Architecture of the human cerebral cortex. Regional and laminar organization. In: Paxinos, G.; Mai, JK., editors. The Human Nervous System. Vol. 2. Elsevier; San Diego: 2004. p. 997-1055.

Zilles K, Palomero-Gallagher N. Cyto-, myelo-, and receptorarchitectonics of the human parietal cortex. NeuroImage 2001;14:8–20.

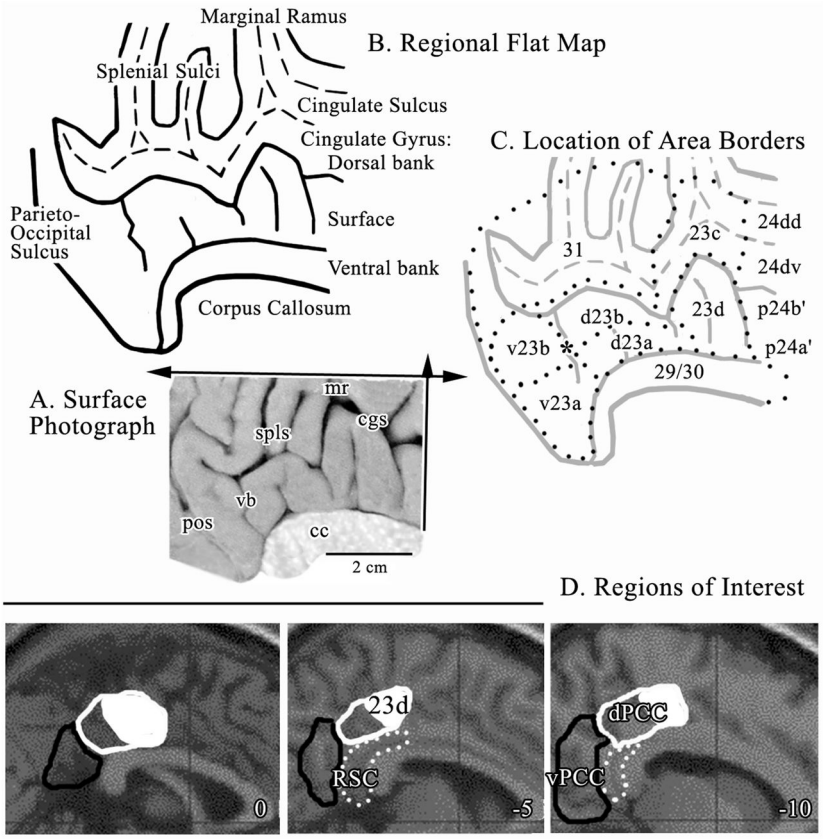

Figure 1.

A. Medial surface photograph with planes of flattening in the dorsal (single arrow) and rostrocaudal (double arrow) orientations. B. Map of flattened sulci and gyri with the dorsal and ventral banks of the cingulate gyrus noted. The fundi of the cingulate and splenial sulci are dashed lines. The retrosplenial areas 29 and 30 were reflected ventrally below the edge of the corpus callosum so as to not interfere with showing area 23. C. Distribution of areas from a histological assessment (dotted lines) including an asterisk over the ventral branch (vb) of the splenial sulci (spls) where the border between areas d23b and v23b was measured for co-registration to standardized maps; also border #4 in Figure 6. The border between dPCC and vPCC is aligned with the vb and centered on the asterisk. D. Regions of Interest outlined in sagittal sections for the MNI brain (coordinates are the distance in mm from the midline) including dPCC (white outlines), area 23d (part of dPCC formed by solid white area inside the white outline), vPCC (black outlines), and retrosplenial cortex (RSC; white dots). cc, corpus callosum; cgs, cingulate sulcus; mr, marginal ramus; pos, parieto-occipital sulcus; spls, splenial sulci; vb, vertical branch of spls.

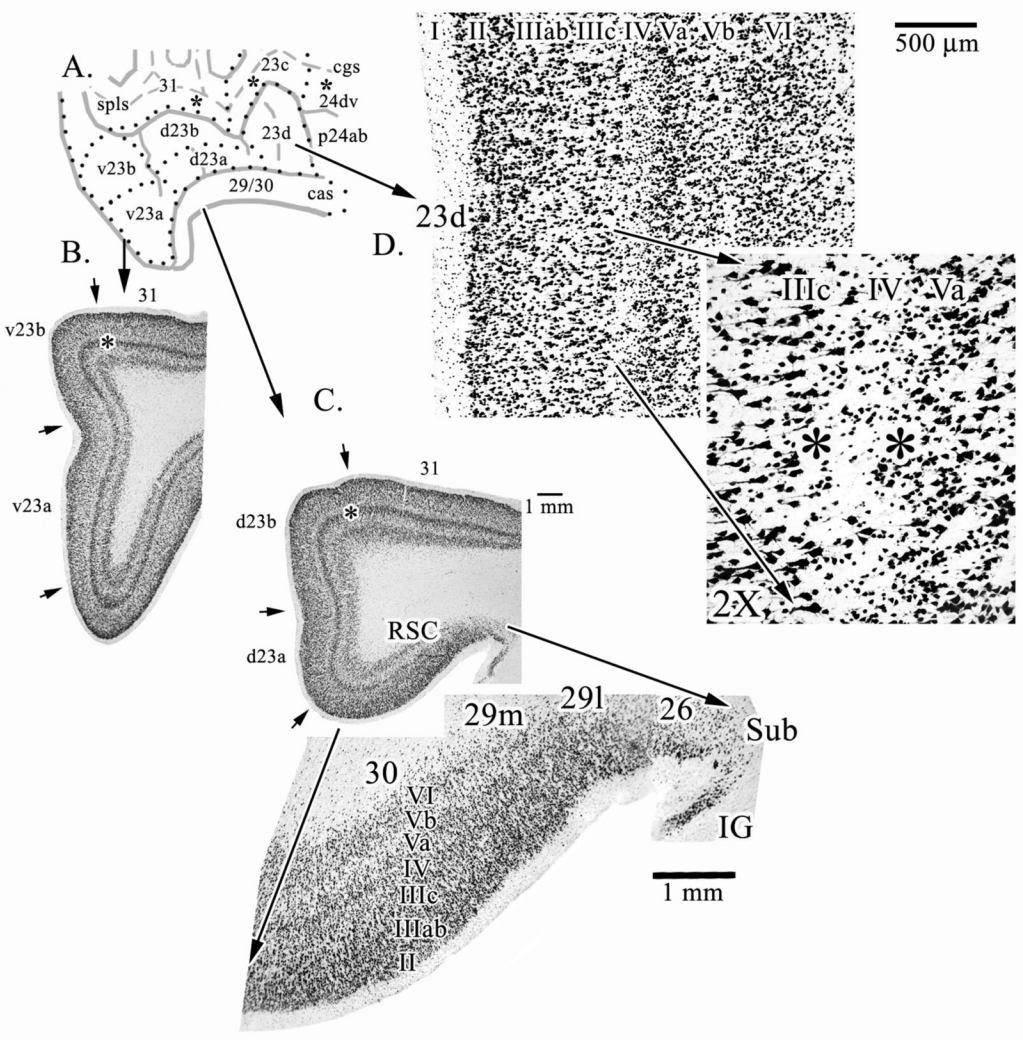

Figure 2.

Overview of key components of the PCC and RSC regions. The three asterisks in the cgs and spls on the line drawing (A.) are where microphotographs were taken for sulcal areas in Figure 4. B. and C. are macrophotographs from levels through v23 and d23, respectively (asterisks emphasize layer Va at this magnification). A pull-out from C. further magnifies the retrosplenial areas 29 and 30 on the ventral bank of the cingulate sulcus. Area 26 is ectosplenial cortex. D. Dysgranular area 23d is shown with a pull-out magnification of a point at which the variability of layer IV (i.e., dysgranularity) is most evident. Between the asterisks it can be seen that layer IV discontinues for a short distance. Sub, dorsal subiculum; IG, indusium griseum.

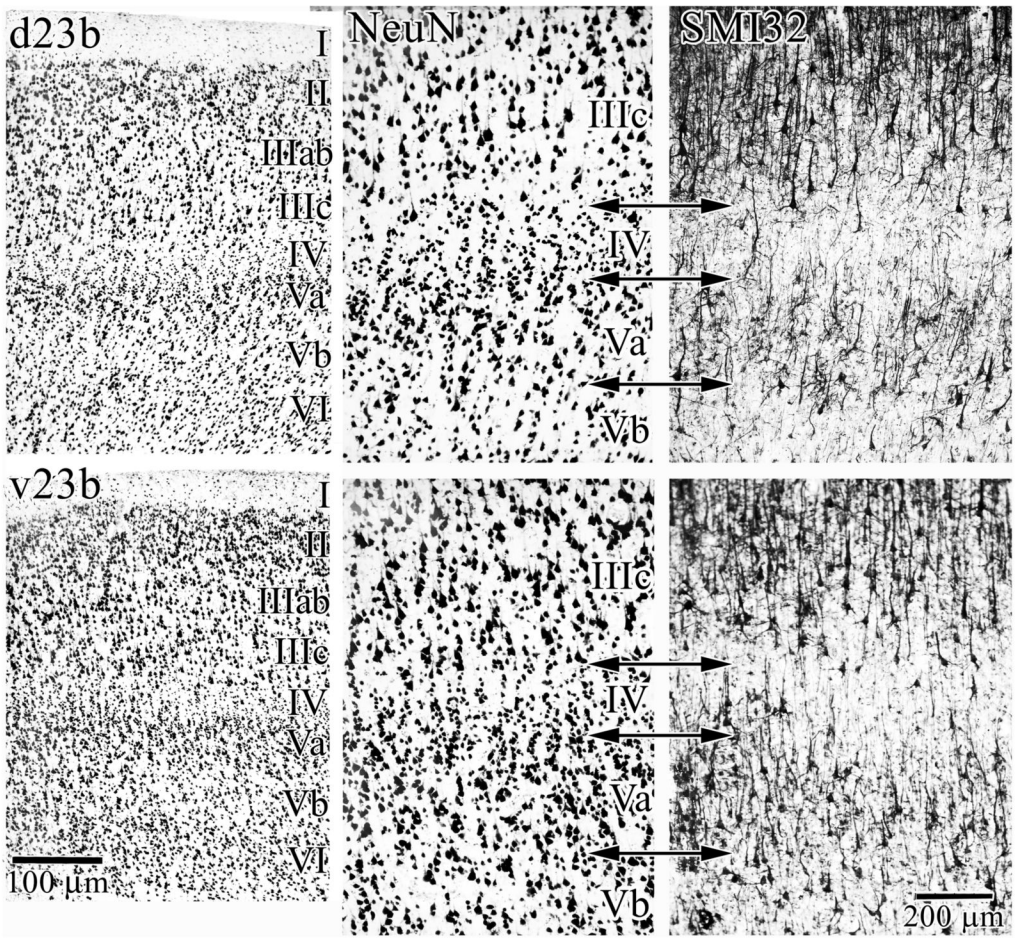

Figure 3.

Cytological details of the dorsal and ventral divisions of area 23b. The breadth and neuron densities in layers II, III, IV, and V are prominent. The density of NFP bearing neurons in layers IIIc, Va, and Vb are greater in v23b than in d23d as shown in the right panels (SMI32). Thus, phenotypic expression of NFP supports the dichotomy of PCC architecture observed in NeuN preparations.

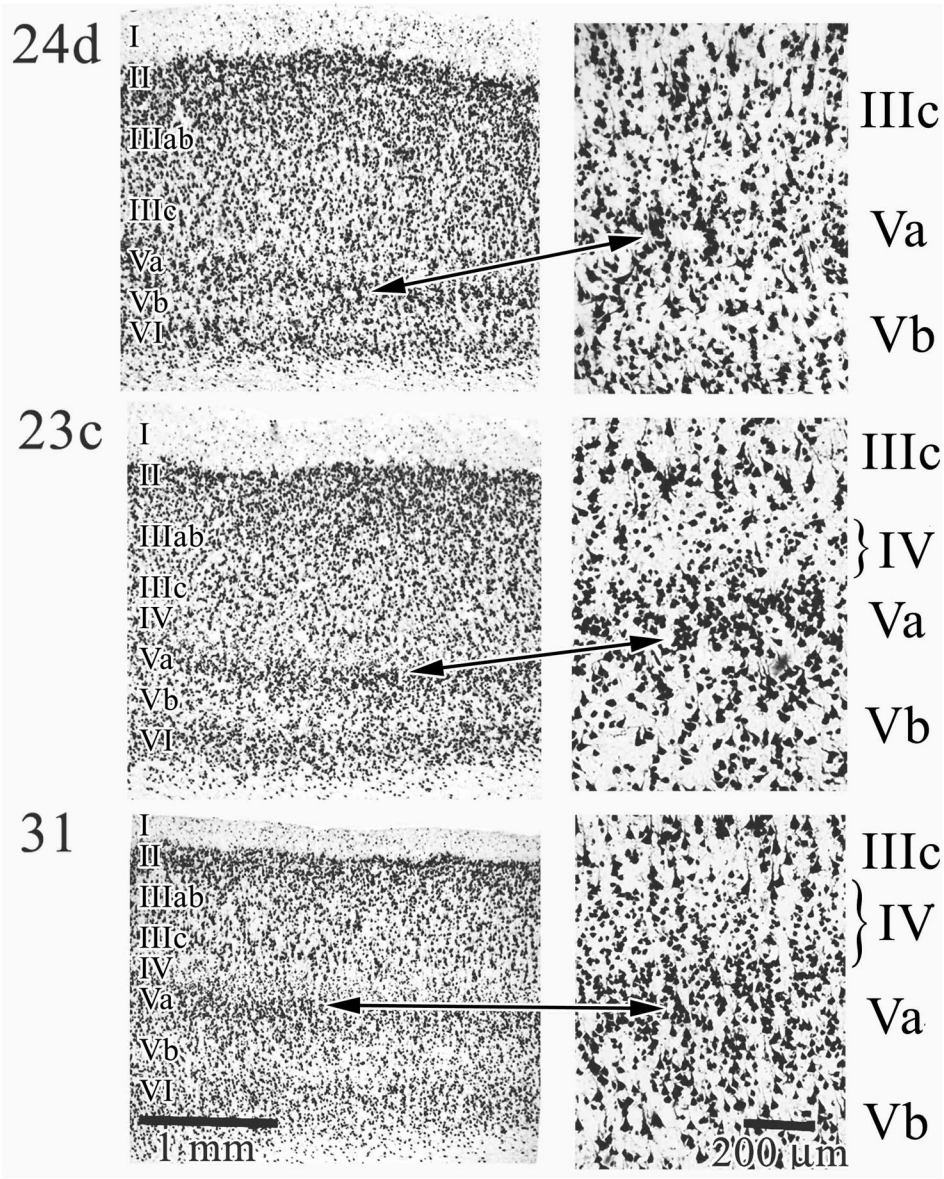

Figure 4.

Cingulate and splenial sulcal areas. Area 24d is provided as a comparison because it is agranular; i.e., lacks a layer IV and layers IIIc and Va directly abut each other. The arrow pair shows exactly which cortex was magnified at the right of the figure. In area 23c layers II–IV are quite broad and layer IV is present though thin. Area 31 has a well developed layer IV and the relative size of layer IIIc is greater than layer Va in contrast to other cingulate areas where there is a relative size equivalency among neurons in these layers. The brackets on layer IV emphasize difference in thickness in all areas.

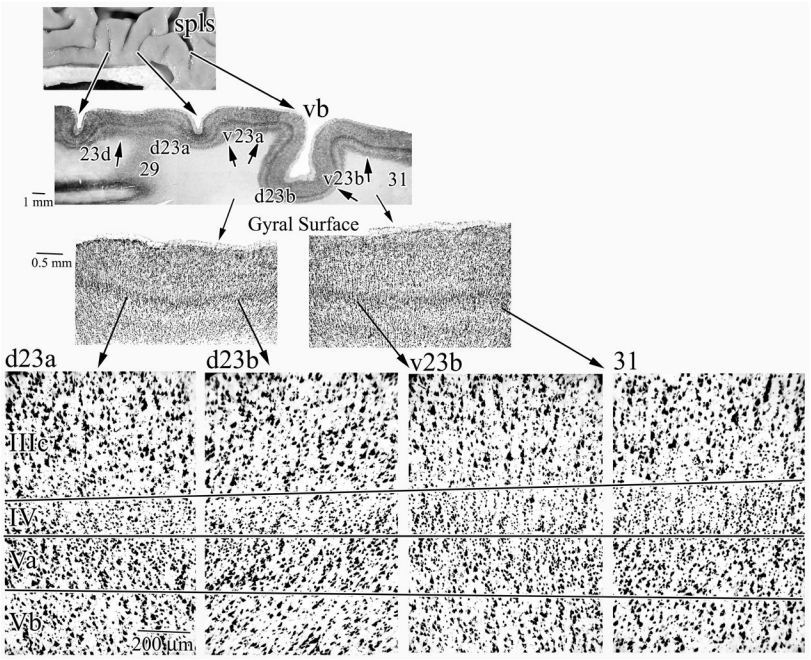

Figure 5.

Horizontal sections show the progressive differentiation of PCC in the rostrocaudal direction. The prominent ventral branch of the spls (vb) is shown in this section and areas d23a, d23b, v23b, and 31 are present. Notice that retrosplenial area 29 is cut with a glancing section at this level and no cytoarchitecture can be differentiated and the level of area 23a is quite dorsal and starting to merge with area 23b and the thickness of layer Va is increased. The highest magnification photographs were aligned on the layer IV/Va border and the other two borders emphasize the striking elaboration of layers IV and Va. Although each panel is a separate photograph, arrows are oriented to mark layer borders so the progressive differentiation of different layers can be compared and appreciated. For example, follow the progressive increase in width and neuron density of layer IV from the left to right of the figure.

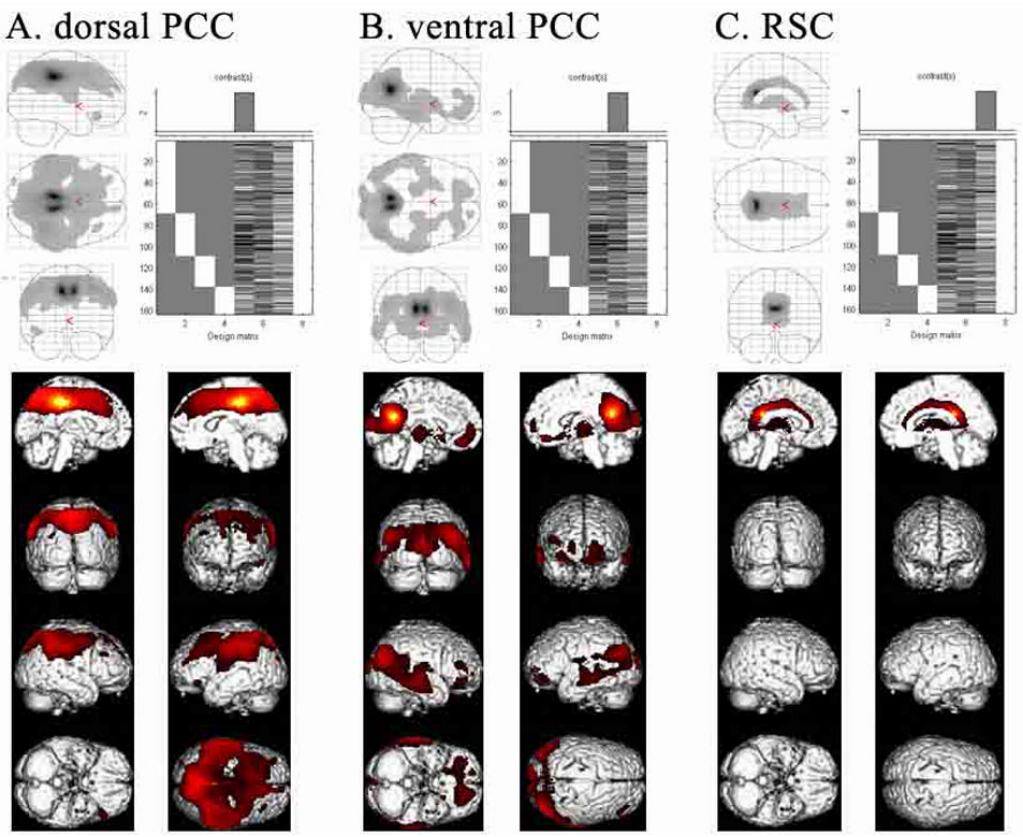

Figure 6.

ROIs based on histological assessment and co-registration (Fig. 1D) were used to evaluate CMRGlu in the resting state for 163 cases. SPM results were considered significant and are shown at false discovery rate (FDR)-corrected p value <0.001 for A. dPCC, B. vPCC, and C. RSC. The identified correlated voxels for each ROI suggest very different functional connectivity for each ROI.

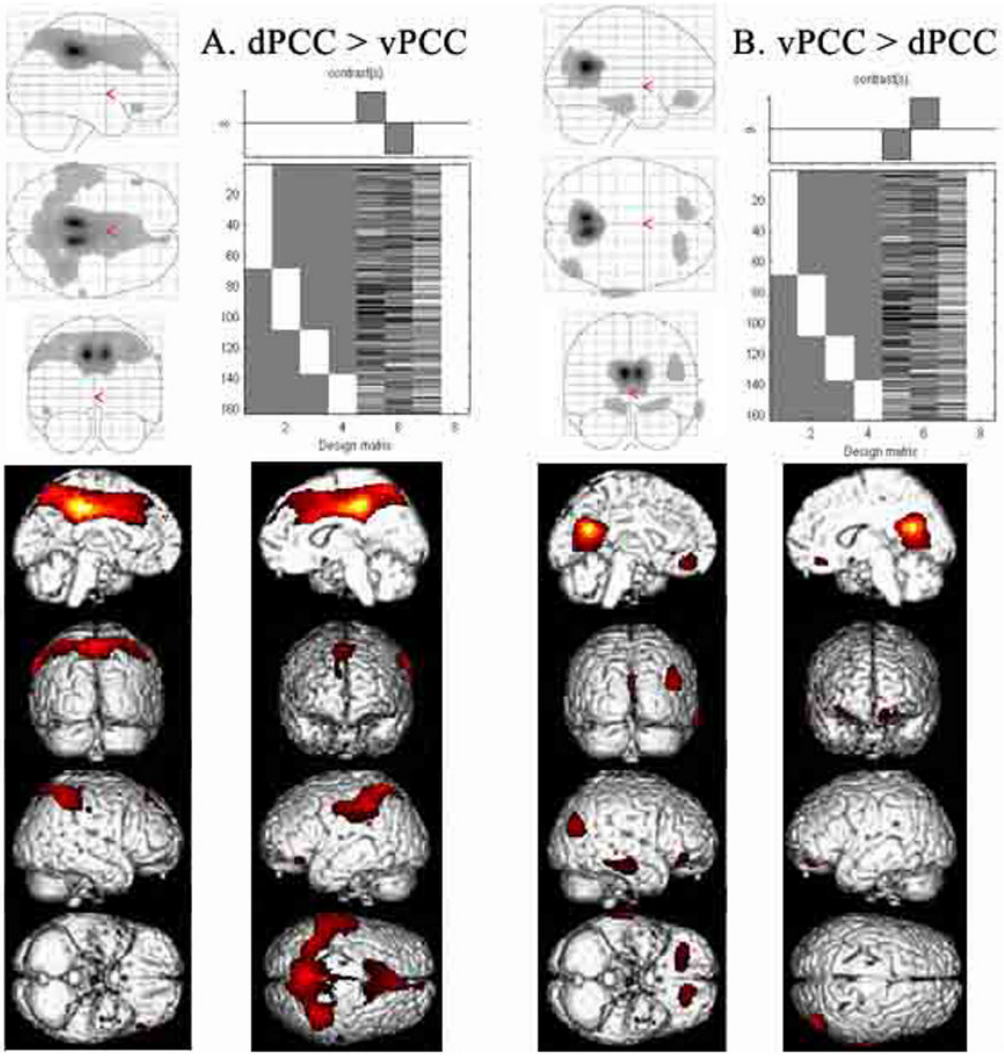

Figure 7.

Validation of the correlation analysis was performed by directly comparing bCCOI for each division of PCC to determine the level of significant difference between the two bCCOI. There is a reduction of medial prefrontal activity in dPCC and of posterior parietal activity in vPCC suggesting some functional overlap in these two regions. The thalamic site in vPCC is lost following interaction analysis with dPCC suggesting, that although thalamic activity was not observed in the dPCC correlations (Fig. 6), some may be present at a subthreshold level.

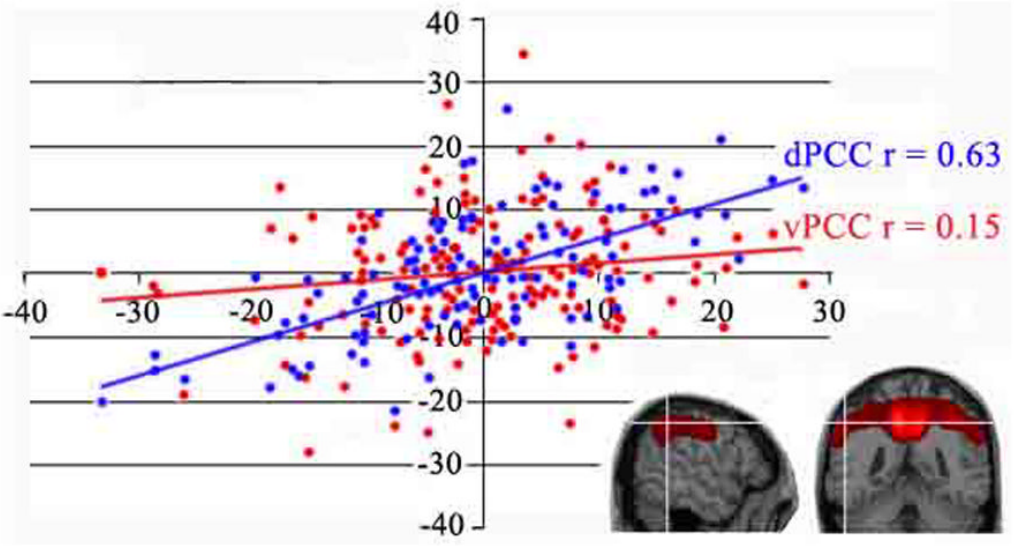

Figure 8.

Plot of the regression between rCMRGlu in parietal cortex (x, y, z coordinates; −54, −44, 44 mm). Location of the parietal voxel is shown for two planes of section at the white cross hairs. A significant correlation is shown with dPCC but not for vPCC. Each dot represents one subject.

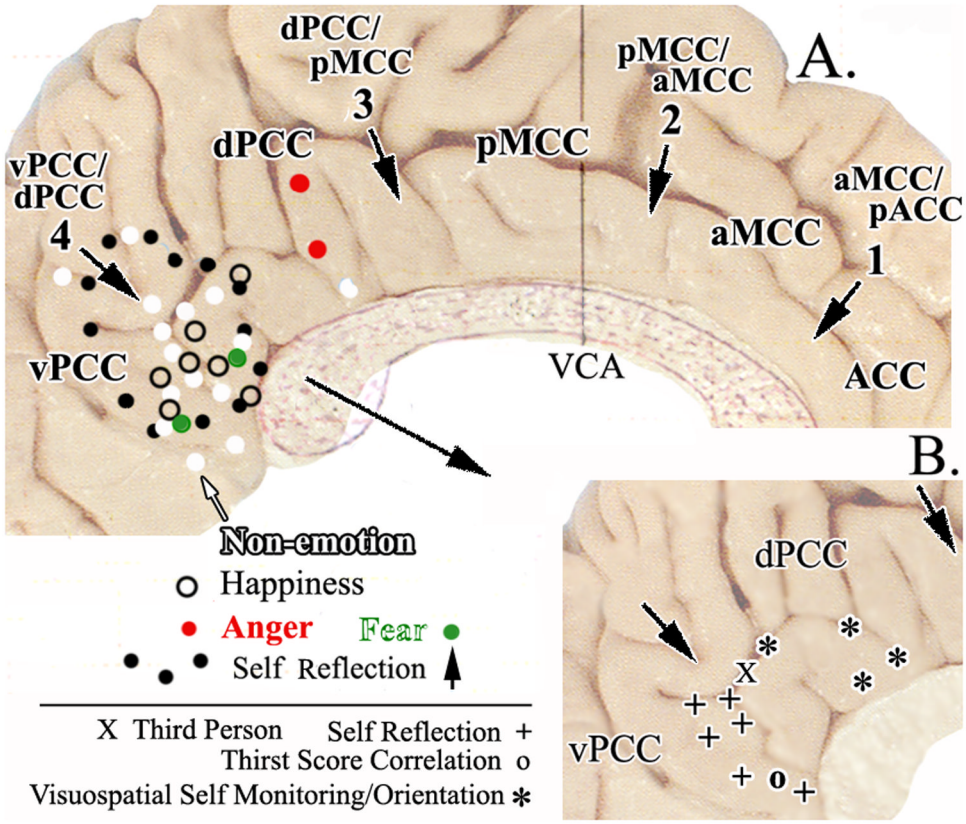

Figure 9.

The four cingulate regions and their borders are shown with arrows and bold print in A (VCA, vertical plane at the anterior commissure). Activations associated with three simple emotions (happiness, anger, fear) generated with scripts or faces are shown as are those associated with non-emotional scripts and faces with symbols for peak activation sites discussed in the text. Overlap of emotional and non-emotional information processing suggests that vPCC has a nonspecific role in emotion that is not the case for subgenual ACC. A. also shows differentiation within PCC with the full area of activation in a study of self-reflection (black dots; Johnson et al., 2002). B. Pull out of the posterior cingulate region with locations of peak-voxel activations during self-reflection, third-person vs first person, and visuospatial self monitoring and orientation.

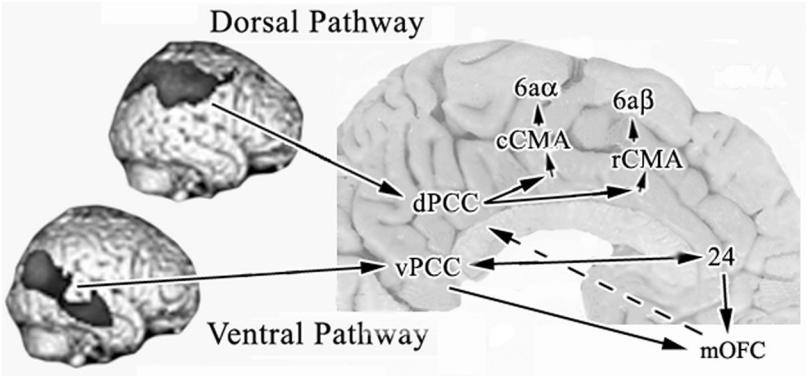

Figure 10.

Differential information processing through the dorsal and ventral visual pathways to PCC based on presented human bCCOI and previous monkey corticocortical connection studies. A key function of PCC is in visuospatial orientation and visual processing pathways are preserved into PCC according to the bCCOI analysis. A circuit hypothesis of the flow of information through the cingulate gyrus is suggested to the rostral and caudal cingulate motor areas (rCMA, cCMA) to account for differences in functional activity for the two divisions of PCC and a terminal synthesis of information from the vPCC and ACC to medial orbitofrontal cortex (mOFC). A link to premotor systems (dashed arrow) is suggested by bCCOI in OFC with the dPCC ROI.